Plant Physiology and Biochemistry 207 (2024) 108364

Contents lists available at ScienceDirect

Plant Physiology and Biochemistry

journal homepage: www.elsevier.com/locate/plaphy

Proximate biomass characterization of the high productivity marine microalga *Picochlorum celeri* TG2

Alaina J. LaPanse [a,*], Anagha Krishnan [a], Galen Dennis [a], Devin A.J. Karns [a], Lukas R. Dahlin [b], Stefanie Van Wychen [c], Tyson A. Burch [a], Michael T. Guarnieri [b], Joseph C. Weissman [a], Matthew C. Posewitz [a]

[a] Department of Chemistry, Colorado School of Mines, Golden, CO, 80401, USA
[b] Biosciences Center, National Renewable Energy Laboratory, Golden, CO, 80401, USA
[c] Renewable Resources and Enabling Sciences Center, National Renewable Energy Laboratory, Golden, CO, 80401, USA

ARTICLE INFO

Handling Editor: Dr. Mario De Tullio

Keywords:
Microalgae
Biomass composition
Marine
Nitrogen deplete
High productivity

ABSTRACT

Microalgae are compelling renewable resources with applications including biofuels, bioplastics, nutrient supplements, and cosmetic products. *Picochlorum celeri* is an alga with high industrial interest due to exemplary outdoor areal biomass productivities in seawater. Detailed proximate analysis is needed in multiple environmental conditions to understand the dynamic biomass compositions of *P. celeri*, and how these compositions might be leveraged in biotechnological applications. In this study, biomass characterization of *P. celeri* was performed under nutrient-replete, nitrogen-restricted, and hyper-saline conditions. Nutrient-replete cultivation of *P. celeri* resulted in protein-rich biomass (~50% ash-free dry weight) with smaller carbohydrate (~12% ash-free dry weight) and lipid (~11% ash-free dry weight) partitions. Gradual nitrogen depletion elicited a shift from proteins to carbohydrates (~50% ash-free dry weight, day 3) as cells transitioned into the production of storage metabolites. Importantly, dilutions in nitrogen-restricted 40 parts per million (1.43 mM nitrogen) media generated high-carbohydrate (~50% ash-free dry weight) biomass without substantially compromising biomass productivity (36 g ash-free dry weight m^{-2} day^{-1}) despite decreased chlorophyll (~2% ash-free dry weight) content. This strategy for increasing carbohydrate content allowed for the targeted production of polysaccharides, which could potentially be utilized to produce fuels, oligosaccharides, and bioplastics. Cultivation at 2X sea salts resulted in a shift towards carbohydrates from protein, with significantly increased levels of the amino acid proline, which putatively acts as an osmolyte. A detailed understanding of the biomass composition of *P. celeri* in nutrient-replete, nitrogen-restricted, and hyper saline conditions informs how this strain can be useful in the production of biotechnological products.

1. Introduction

Global climate patterns have shifted in the 21st century following decades of anthropogenic greenhouse gas emissions (Lynas et al., 2021). Such changes have resulted in more frequent and extreme natural disasters including droughts, floods, hurricanes, heat waves, wildfires, and severe storms (Fawzy et al., 2020). Fossil fuel-driven manufacturing processes pose a two-fold risk: both the emission of greenhouse gasses which contribute to climate warming, and the generation of petroleum-derived plastic products and waste which can become toxic and are poorly reversible (Macleod et al., 2021). To mitigate the impacts of climate change and non-biodegradable waste products, renewable energy and product platforms are required. Microalgae are relatively efficient primary producers of valuable constituents including lipids, carbohydrates, proteins, and pigments that can be used for biofuels (including sustainable aviation fuel; SAF) and other bioproducts (Barbosa et al., 2023; Foley et al., 2011; Ruiz et al., 2016; Work et al., 2013).

Several species of *Picochlorum* are of interest due to their fast outdoor growth and high areal productivities in seawater, with *Picochlorum celeri* TG2 achieving over 40 g AFDW m^{-2} day^{-1} outdoor productivities on peak days (~31 g AFDW m^{-2} day^{-1} average) during summer cultivation in Mesa, Arizona (Krishnan et al., 2021). Genetic engineering tools were developed for multiple *Picochlorum* spp. to enable targeted strain engineering approaches (Dahlin and Guarnieri, 2021, 2022; Krishnan et al.,

* Corresponding author.
E-mail address: alapanse@mines.edu (A.J. LaPanse).

https://doi.org/10.1016/j.plaphy.2024.108364
Received 1 September 2023; Received in revised form 23 December 2023; Accepted 10 January 2024
Available online 11 January 2024

2020, 2023). Recent work from Dahlin et al. (2019) has identified the major biomass constituents of *Picochlorum renovo*, and work from Barten et al., 2020) has identified replete biomass partitioning of *Picochlorum* sp. (BPE23); however, a detailed proximate characterization of *Picochlorum celeri* under diverse, deployment-relevant cultivation conditions has yet to be reported (Barten et al., 2020; Dahlin et al., 2019).

To maximize the value of microalgal biomass by informing optimal cultivation regimes, thorough proximate characterization of industrial microalgal strains is necessary. It is widely observed that microalgal biomass shifts as cells adapt to changing environmental conditions, including changes in nitrogen availability and salinity (Newell Arber, 1901; Procházková et al., 2014). Even under similar culturing conditions, microalgal strains will often show differences in composition partitioning, reflective of unique lineages and regulatory components; resulting in strains with differing cell walls, photosynthetic antennae, and cell storage products (Finkel et al., 2016).

Despite strain specific variability, biomass partitioning trends can be observed within broad classes of microalgae under varying nutrient conditions. High protein biomass fractions are often observed in microalgae when averaging over all growth stages. As evaluated by Gatenby et al. (2003), both green and diatom microalgae contained an average of 45%–55% total protein. Additionally, carbohydrate content was highly variable depending upon growth stage, with carbohydrates increasing in later growth stages due to nutrient limitation. Lipid content may also increase during stationary phase when acting as a cellular storage product, as shown in *Neochloris oleabundans* (Gatenby et al., 2003). Accumulation of either lipids or carbohydrates because of nutrient limitation is commonly observed in microalgae, as these components are storage metabolites that help cells survive (Ran et al., 2019). When cultivated industrially, intentional dosage and restriction of nutrients is a useful strategy for directing biomass composition towards carbon storage products. For a cultivation strategy of nutrient management to be successfully applied, a detailed analytical characterization of the proximate biomass composition of a given microalgal strain is necessary.

Analytical methods for the quantification and evaluation of plant biomass components have been utilized for the better part of a century (Dreywood, 1946; Luzon, 1948; Morris, 1948). Microalgal biomass composition has been of interest for nearly as long, with initial analytical methods accounting for most major components including nucleic acids, pigments, lipids, proteins, and carbohydrates (Ricketts, 1966). Several common methods are typically used to characterize microalgal biomass components. Total protein is readily quantified colorometrically using a Lowry-type method (Lowry et al., 1951). Although this protocol has been widely utilized in microbiology for decades, monomer identification requires detailed amino acid analysis. For the quantification of microalgal lipids, conversion to fatty acid methyl esters (FAMEs) followed by GC-FID analysis is well validated (Laurens et al., 2014; Work et al., 2010). As with total protein measurements, a common total carbohydrate assay uses the anthrone reagent to colorometrically quantify monomeric reducing carbohydrates (Finkel et al., 2016; Mayorga et al., 2021; Morris, 1948; Viles and Silverman, 1949). Following hydrolysis of complex carbohydrates, monomeric carbohydrate data can be determined through monosaccharide chromatography. Even when conducting thorough biomass proximate analysis, a complete characterization of all biomass constituents is not often achieved. While unknown biomass components remain, literature suggests that this fraction is likely composed of small polar metabolites, vitamins, carotenoids, and uncaptured lipids, proteins, and carbohydrates (Van Wychen et al., 2021). Recent work from Laurens et al. has highlighted the need for detailed, verifiable proximate characterization of algal biomass. When comparing several methods for protein, lipid, and carbohydrate quantification, relative standard deviations up to 20% have been reported (Laurens et al., 2012a). Such variability illustrates the utility of several orthogonal methods for each biomass component.

In this study, an initial characterization of the biomass composition of the industrially relevant alga *Picochlorum celeri* TG2 was performed. Major biomass components including carbohydrates, proteins, lipids, pigments, and nucleotides were measured under nutrient-replete, nitrogen-restricted, and hyper-saline (2X sea salts) conditions. Furthermore, amino acid analysis (AAA), FAME analysis, and monosaccharide analysis were performed to observe monomeric changes in major biomass components following media variation. These data provide insights into the relevance of *P. celeri* for the production of renewable products from microalgal biomass components, which include polymers, fuels, feed/food constituents, biomaterials, and nutritional and cosmetic supplements from the proteins, carbohydrates, lipids and pigments of algal biomass. Moreover, these efforts rationally inform cultivation regimes to maximize carbon flux to algal biomass targets.

2. Materials and methods

2.1. Cultivation conditions

Picochlorum celeri TG2 was cultivated in filter sterilized nutrient-replete sea salt medium similar to that described by Weissman et al. (2018); Weissman et al. (2018). Specifically, marine salinity was obtained through the addition of 40 g L^{-1} Instant Ocean® (Spectrum Brands, USA); major nutrients included iron (0.0150 g L^{-1} $FeSO_4*7H_2O$), phosphate (0.0890 g L^{-1} KH_2PO_4), and nitrogen (0.436 g L^{-1} urea = 0.204 g L^{-1} N = 200 ppm (parts-per-million) N); trace metals were included ($3.14*10^{-4}$ g L^{-1} $MnSO_4*1H_2O$, $2.42*10^{-5}$ g L^{-1} $CoCl_2*6H_2O$, $4.88*10^{-5}$ g L^{-1} $ZnSO_4*7H_2O$, $2.00*10^{-6}$ g L^{-1} $CuSO_4*5H_2O$, $6.81*10^{-6}$ g L^{-1} $Na_2MoO_4*2H_2O$); EDTA (0.0203 g L^{-1} EDTA) was used to chelate metals; vitamins consisted of ($1.54*10^{-3}$ g L^{-1} thiamine HCl, $4.40*10^{-6}$ g L^{-1} biotin, and $4.40*10^{-6}$ g L^{-1} cyanocobalamin). The nutrient-replete medium is ~40 ppt (parts-per-day--thousand) Instant Ocean marine salts, 200 ppm N, and is used as the control.

As summarized in Fig. 1, for nutrient-replete, gradually nitrogen-depleted, and hyper- (2X sea salts) saline experiments, *P. celeri* was cultivated at a volume of 400 mL in 500 mL square bottles (Pyrex, Germany) within a custom built, solar-simulating, three-station bioreactor. Gas levels were controlled using mass-flow controllers (Sierra Instruments, USA) with each 400 mL culture receiving a continuous supplementation of humidified 400 SCCM filtered air and 9 SCCM carbon dioxide through a coarse cylindrical gas sparger (Chemglass Life Sciences, USA). Continuous culture mixing was achieved using magnetic stirring (Thermo Fisher Scientific, USA). Diel lighting of the cultures was provided along the flat rear surface of the bottle using custom-built 5000K LED light panels. Light output was tuned to mimic solar emission and controlled using a diel script simulating a cloudless summer day in the western United States, with a maximum intensity of 2200 PAR [calibrated in water using a spherical light sensor (Walz, Germany)], and ~10 h of darkness. Culture temperature was maintained at 33 °C using a Peltier module (Analog Technologies, USA) beneath the bottle to heat and cool the culture to the set point. Manual dilutions were performed once per day immediately following sunset, with makeup water added to account for evaporative loses prior to dilution in sea salt media. Proximate analysis samples were obtained (following makeup water addition but prior to dilution in media) on day 3 of steady-state, nutrient-replete growth after sunset, with biomass samples preserved frozen at −80 °C as whole culture or pellets, as indicated.

For gradual nitrogen-depletion experiments, cultures were maintained as described above; however, 60% dilutions (60% culture volume removed) were performed daily for 3 days in biological triplicate using nitrogen-free sea salt medium to induce severe nitrogen restriction by Day 3. Proximate analysis samples were obtained daily, after sunset prior to dilution, to document changes in biomass composition as a result of increasingly severe nitrogen depletion. For hypersaline (2X sea salt) experiments, cultures were maintained as above in 2X (80 ppt Instant Ocean) sea salt medium in biological duplicate for 3 days with

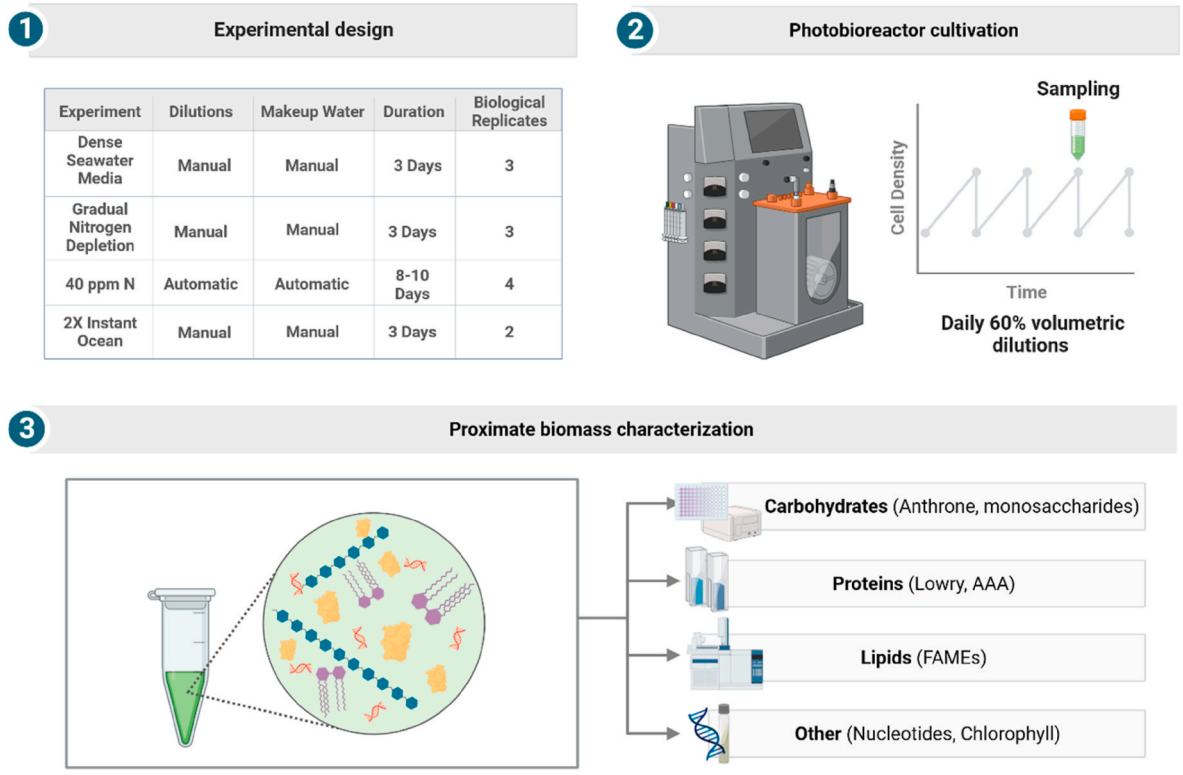

Fig. 1. Schematic representation of experimental design, bioreactor cultivation, and proximate analysis of *Picochlorum celeri* in sea salt media, under gradual nitrogen depletion, 40 ppm N restriction, and 2X Instant Ocean (sea salt) media.

60% volumetric dilutions each day. On days 2 and 3 of steady-state cultivation, proximate analysis samples were obtained after sunset prior to dilution to provide duplicate replicates.

For 40 ppm N restricted experiments, *P. celeri* was cultivated in biological quadruplicate in an automated bioreactor similar to those previously described (Cano et al., 2021). Automated culturing conditions allowed for the addition of makeup water every 2 h throughout the day to compensate for evaporation. Automated batch dilutions (60% volumetric dilution in nutrient-dense sea salt media containing 40 ppm N) and sampling were performed daily 1 h before sunset using peristaltic pumps (Watson-Marlow, UK). A load cell (Mettler Toledo, USA) beneath the bottle measured culture volume removed and sterile media added through autoclaved lines and 0.1 μm inlet filters. Proximate analysis samples were obtained daily as indicated along with AFDW measurements (see Table S1) during steady-state cultivation prior to dilution 1 h before sunset.

2.2. Biomass and productivity calculations

Biomass productivity was determined using ash-free dry weight (AFDW) measurements. TCLP Glass Fiber Filters (Cytiva, USA (formerly Pall Lab), 4.7 cm diameter, 0.7 μm) were pre-ashed at 550 °C for 15–20 min to remove carbon contaminants. Sufficient (>7 mL) *P. celeri* biomass was filtered onto pre-ashed filters and washed with 20 mL 0.5 M ammonium formate to remove salts. After washing, filters were dried overnight at 105 °C and biomass dry weight was measured. Filters were then heated for >1 h at 550 °C, and remaining ash was gravimetrically measured. AFDW measurements were obtained by subtracting the ash measurement from the biomass dry weight (Breuer et al., 2012). All AFDW measurements were performed in technical duplicate.

Biomass productivity was reported using AFDW measurements over several days and averaged among replicates (as shown in Fig. 1, Figs. S1–3, Table S1) with error reported as ± 1 standard deviation. Biomass productivity was calculated as the difference between the starting, immediately after dilution, AFDW and final, immediately prior to dilution, AFDW multiplied by the culture volume to illuminated surface area ratio for the culture bottles, resulting in productivity in g AFDW m^{-2} day^{-1} (Weissman et al., 2018). Starting AFDW was calculated using final AFDW measurements and measured culture volumes. Final AFDW was measured as described above.

2.3. Protein measurements

Total protein measurements were obtained using a modified Lowry assay and amino acid analysis (AAA). For the modified Lowry assay, 0.5 mL cell pellets were maintained at −80 °C. 1.0 mL of lysis buffer comprised of 50 mM Tris-HCl pH 8, 75 mM NaCl, 5% glycerol, and 1% SDS was used to resuspend cell pellets in 0.5 mL (Lowry et al., 1951). Resuspended samples were kept on ice and probe sonicated using a VirSonic 475 (Virtis, USA) at an intensity of 3 for 2 min in ice water, with two rounds of sonication performed on each sample. Samples were then placed immediately into boiling water for exactly 2 min. After boiling, SDS was allowed to precipitate on ice (~20 min). Once precipitated, samples were centrifuged at 15,000 RPM, 4 °C for 10 min. The supernatant was then analyzed using the Bio-Rad DC (Bio-Rad, USA) modified Lowry protein assay kit per manufacturer's instructions and measured in 1 cm cuvettes at 750 nm using a spectrophotometer. 10 mg/mL stock bovine serum albumin (BSA) in lysis buffer was used to create a standard curve of 0, 0.1, 0.2, 0.4, 0.8, and 1.6 mg/mL. Final unknown sample concentration was calculated using the linear best fit of the BSA standard curve.

AAA was performed at the University of California, Davis Molecular Structure Facility as a fee-for-service data set. To determine and quantify (within 100 pmol) individual amino acids, 3 Hitachi (L-8800, L-8800a, L-8900) amino acid analyzers are employed. These analyzers use ion-exchange chromatography to separate amino acids followed by ninhydrin reaction prior to detection (Cooper et al., 2000).

2.4. Lipid measurements

Total lipid measurements were obtained through fatty acid methyl ester (FAME) analysis by gas chromatography-flame ionization detection (GC-FID). FAME measurements were conducted using two separate methods as published by Work et al. and Laurens et al. for validation (Laurens et al., 2012b; Work et al., 2010).

For the former, 0.5 mL of liquid culture was frozen and stored at −80 °C. 1 mL methanol saturated with sodium hydroxide was used for saponification and acid-catalyzed methylation was achieved using 1.5 mL of methylation reagent (14.6 mL 12 N HCl + 235.4 mL MeOH) incubated overnight at 60 °C. FAMEs were extracted using 1.25 mL n-hexane inverted at room temperature for 30 min, then analyzed by GC-FID using an Agilent 7890A gas chromatograph with a HP-Innowax 19091N-133 column (Agilent Technologies, USA). All runs included a Supelco 37 component FAME standard (Sigma-Aldrich, USA) and a C13 fatty acid internal standard for instrument validation and total FAME quantification (Work et al., 2010). GC-MS analysis was used to validate GC-FID assignments. This was performed using a 7890B Gas Chromatography System with a HP-Innowax 19091N-133 column (Agilent Technologies, USA), followed by mass spectrometry using a 5977B Quadrupole Detector (Agilent Technologies, USA).

For the latter, 100 mg or greater of lyophilized biomass was stored at −80 °C. For each sample 5–10 mg of lyophilized biomass was transesterified using 200 μL chloroform:methanol (2:1, v/v) and 300 μL 0.6M hydrochloric acid:methanol for 1 h at 85 °C. FAMEs were extracted using 1 mL hexane and analyzed on an Agilent 7890A GC-FID equipped with an Agilent J&W GC Column DB-Wax length 30 m, internal diameter 0.25 mm, film thickness 0.25 μm (Agilent Technologies, USA). All runs included a NuChek 461C Working Solution FAME standard (Nu-Chek Prep, Inc., USA) and a C13 hydrocarbon internal standard for validation and total FAME quantification (Laurens et al., 2012b).

2.5. Carbohydrate measurements

Total carbohydrate measurements were obtained using an anthrone assay. 0.5 mL of liquid culture was maintained at −80 °C. A standard curve was prepared using D-glucose at concentrations of 0, 25, 50, 75, 100, 150, 200, 300, 400, 500 mg/L 100 μL of thawed liquid culture or standard was mixed with 900 μL of cold anthrone reagent (2 g L^{-1} anthrone, 71% 10 N H_2SO_4 + 29% H_2O v/v) and boiled for 12 min in a water bath. Immediately following boiling, tubes were cooled in an ice bath to halt color development in the anthrone reagent, then absorbance was measured at 625 nm in a spectrophotometer using 1 cm cuvettes. Unknown sample concentrations were calculated using the linear best fit equation from the D-glucose standard curve (Luzon, 1948; Morris, 1948; Viles and Silverman, 1949).

Monosaccharide quantification was conducted as previously described (Dahlin et al., 2018). Briefly, 25 mg of lyophilized biomass was hydrolyzed by 250 μL of 72% (w/w) sulfuric acid at 30 °C for 1 h, then diluted in 7 mL of water and autoclaved for 1 h at 121 °C. Lysate was filtered through a 0.2 μm nylon filter, and monosaccharides were isolated using high pressure anion exchange liquid chromatography with pulsed amperometric detection using a CarboPac PA1 column (Thermo Fisher Scientific, USA) on a Dionex ICS-5000+Analytical HPIC System. A calibration standard was prepared containing D(+)glucose (cat G7528; Sigma Aldrich, USA), D(+)xylose (cat X3877; Sigma Aldrich, USA), D(+)galactose (cat G0750; Sigma Aldrich, USA), L(+) arabinose (cat 10839; Sigma Aldrich, USA), D(+)mannose (cat 63579; Sigma Aldrich, USA) (Van Wychen et al., 2021).

Starch quantification was done as described previously using a Starch (HK) Assay Kit (Sigma-Aldrich, USA) (Posewitz et al., 2004). Briefly, 10 mL of *P. celeri* culture was pelleted for 10 min at 4000 *rcf* then stored at −20 °C until assay. Pigments were extracted in 10 mL of 100% MeOH, the culture was pelleted again via centrifugation, and the supernatant was removed. The cell pellet was resuspended in 1.0 mL 100 mM sodium acetate pH 4.5 and probe sonicated using a VirSonic 475 (Virtis, USA) at an intensity of 3 for 2 min for cell lysis. The sample was boiled for 3 min (per Sigma-Aldrich protocol), the volume was increased to 25 mL using deionized water, then autoclaved for 1 h at 135 °C. Deionized water was used to increase sample volume to 100 mL, then the manufacturer's protocol was followed for the starch and glucose assays. Final absorbance at 340 nm was measured in 1 cm quartz cuvettes in a spectrophotometer.

2.6. Nucleic acid measurement and calculations

Total nucleotides comprised the sum of total RNA and total DNA. Total RNA was measured using a phenol:chloroform extraction using TRI Reagent (Zymo Research, USA) and a standard protocol (Thermo Fisher Scientific, USA). Briefly, 0.25 mL of cells were pelleted at 8000 g for 5 min, resuspended in 0.75 mL TRI Reagent, and incubated at room temperature for 5 min. 0.15 mL of chloroform was added and samples were incubated at room temperature for 3 min then centrifuged at 12,000 g at 4 °C for 15 min. The upper aqueous phase containing RNA is removed via micropipette. 0.375 mL isopropanol is added to the aqueous phase and incubated for 10 min at 4 °C, then centrifuged for 10 min at 12,000 g and 4 °C. The RNA forms a pellet which is then washed with 0.75 mL 75% ethanol and air dried for 10 min. The pellet is resuspended in RNAse-free water and absorbance is measured at 230 nm, 260 nm, and 280 nm using a NanoDrop (Thermo Fisher Scientific, USA) (Chomczynski and Sacchi, 1987). Total DNA was estimated using flow cytometry total cell count measurements, average nucleotide base pair weight, and number of total genomic base pairs (Becker et al., 2020; Dolezel et al., 2003). Therefore, total DNA content (pg) was the quotient of the genome size (bp) and the average nucleotide base pair weight (0.978×10^9 pg) multiplied by the total number of cells.

2.7. Chlorophyll measurements

Chlorophyll content was determined using the equations from Porra et al. in methanol. 250 μL of *P. celeri* culture was centrifuged at maximum speed (20,000 g) for 5 min at 4 °C. The supernatant was removed and the cell pellet was resuspended in 1 mL of 100% methanol followed by vortexing at maximum speed for 1 min. The sample was then centrifuged again at maximum speed for 5 min and absorbance of the supernatant at 665 nm and 652 nm was measured in 1 cm cuvettes using a spectrophotometer (Porra et al., 1989).

2.8. Transmission electron microscopy (TEM)

TEM was performed at the microscopy core facility at the University of Colorado, Boulder. Samples were harvested at the end of the solar day (sunset) on day 3 of gradual nitrogen depletion and after 4 days of the 40 ppm N restriction experiment. Samples (50 mL) were stored on ice for ~1 h during transport to the TEM facility, then high pressure frozen using a Wohlwend Compact O_2 high pressure freezer (Technotrade International, USA), as described previously (Giddings et al., 2017). Frozen specimens were then freeze-substituted in anhydrous acetone containing 2% osmium tetroxide and 0.2% uranyl acetate and embedded in Epon/Araldite resin. Serial thin (80 nm) sections were cut using a Leica UCT ultramicrotome. The serial sections were collected on Formvar-coated copper slot grids, poststained with 2% aqueous uranyl acetate followed by Reynold's lead citrate and imaged using a Tecnai T12 Spirit TEM, operating at 100 kV.

3. Results

3.1. Biomass productivity and proximate composition

When cultivated in a bioreactor with manual dilutions, the average biomass productivity of *P. celeri* in nitrogen-replete, nutrient-dense sea

salt media was 36 ± 4 g AFDW m^{-2} day^{-1}, consistent with daily manual dilutions from prior studies (Weissman et al., 2018). This is similar to productivities when *P. celeri* is cultivated in bioreactors with automated dilutions and regular make-up water additions, resulting in an average productivity of 41 ± 3 g AFDW m^{-2} day^{-1}, consistent with prior studies (Cano et al., 2021; Krishnan et al., 2021, 2023).

Biomass proximate analysis of *P. celeri* resulted in a detailed reporting of carbohydrates, fatty acids, proteins, and chlorophyll under several pond-relevant cultivation conditions. As shown in Fig. 2A, nutrient-replete biomass consisted primarily of protein (51 ± 10% reported from Lowry), carbohydrate (12 ± 2% reported from anthrone) and FAME (11 ± 0.3%) proportions, and smaller amounts of nucleotides (5.7 ± 1%) and chlorophyll (4.4 ± 0.2%). During gradual nitrogen depletion (60% daily dilutions with N-free medium), FAME content was maintained, chlorophyll content decreased, and a large shift was observed from protein-rich biomass (day 0, reported from AAA), to carbohydrate rich biomass (day 3, reported from AAA), as shown in Fig. 2B.

Gradual nitrogen depletion as a result of dilution in N-free sea salt medium shifted biomass to higher carbohydrate levels but also severely decreased culture productivity. Lower levels of N addition were explored in an automated bioreactor to determine whether the carbohydrate fraction could be increased with a minimal reduction in biomass productivity. Daily 60% volumetric dilutions using 40 ppm N sea salt media in place of N-free sea salt medium were performed, followed by an analysis of the biomass composition. Dilutions in 40 ppm N sea salt medium resulted in a similar shift in biomass composition as N-free sea salt medium (carbohydrate reported from anthrone, protein reported from Lowry), as shown in Fig. 2C. However, while biomass productivity following 3 days of gradual nitrogen restriction was near 0 ± 0.4 g AFDW m^{-2} day^{-1} after 3 days (Fig. 2B), sustained biomass productivity in 40 ppm N sea salt medium was 36 ± 0.4 g AFDW m^{-2} day^{-1} (19.3 ± 1.7 g reducing carbohydrates m^{-2} day^{-1}).

Hypersaline (2X sea salt) conditions shifted biomass composition, with more total carbohydrate (22 ± 1% reported from anthrone) and lower chlorophyll (2.1 ± 0.2%) relative to biomass from nutrient-replete cultures, as shown in Fig. 2D (protein reported from AAA).

3.2. Fatty acid methyl esters (FAMEs)

While total FAME content in *P. celeri* biomass remained relatively consistent in all tested conditions, around 11% AFDW, shifts in types of

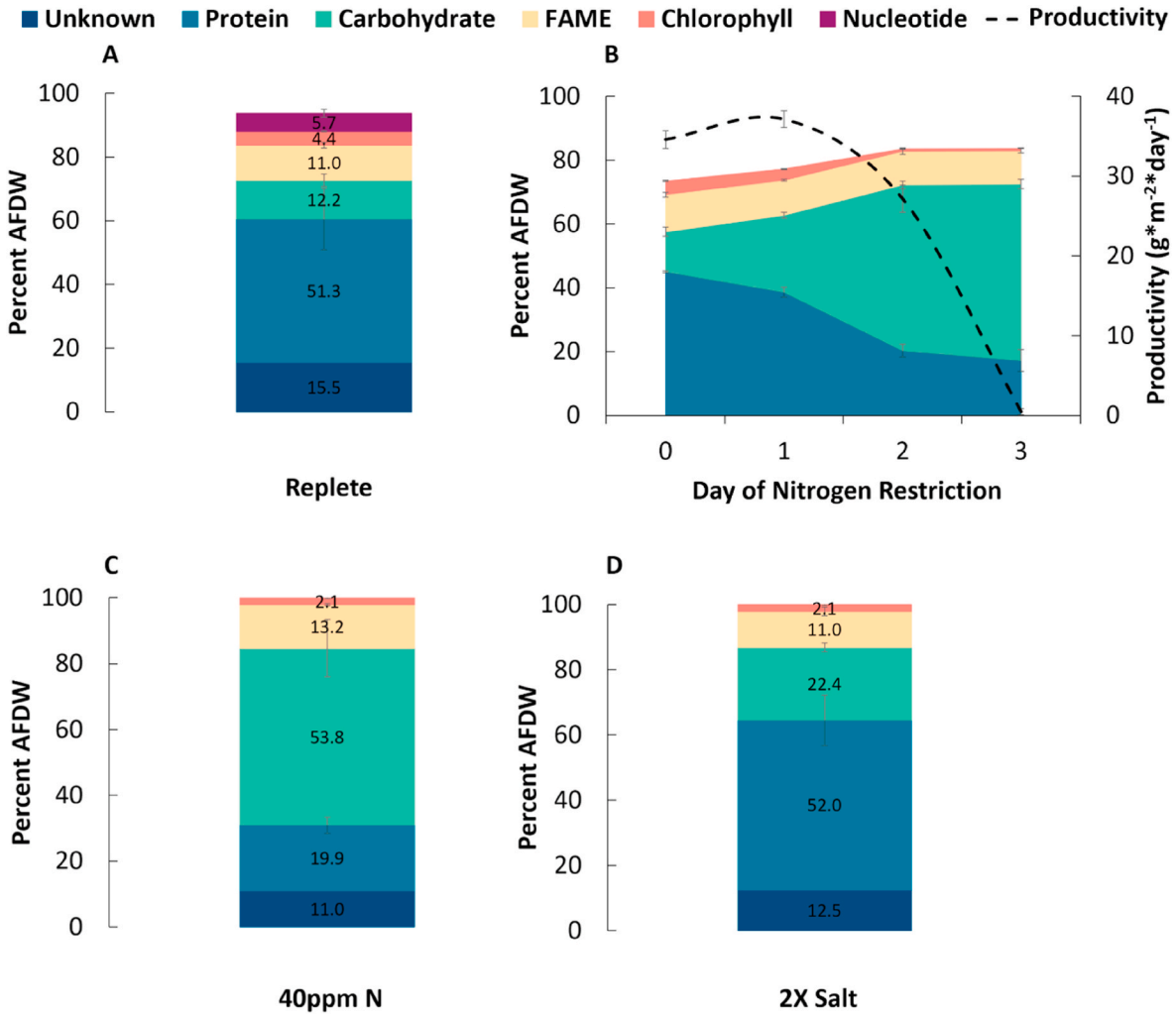

Fig. 2. A. Average biomass composition of *Picochlorum celeri* on day 3 when grown in biological triplicate in nutrient-replete sea salt media in a bioreactor at 33 °C using diel lighting with a 60% volumetric dilution after sunset for 3 days. **B.** Average biomass composition and average productivity of *Picochlorum celeri* grown in biological triplicate in a bioreactor at 33 °C using diel lighting with a 60% volumetric dilution in nitrogen-free media over days 0–3. **C.** Average biomass composition of *Picochlorum celeri* grown in biological quadruplicate in 40 ppm N sea salt media at 33 °C using diel lighting and automated dilutions resulting in a 60% volumetric dilution per day. **D.** Average biomass composition of *Picochlorum celeri* on days 2 and 3 when grown in biological duplicate (4 replicates total) in nutrient-replete 2X (80 ppt) sea salt media in a bioreactor at 33 °C using diel lighting with a 60% volumetric dilution after sunset for 3 days.

cellular fatty acids were noted during nitrogen deprivation. As shown in Fig. 3A, nutrient-replete *P. celeri* biomass had a high ratio of unsaturated fatty acids, primarily C18:3, which was also the highest FAME in abundance under these conditions. C16:0, C18:2, C16:3, C16:1 trans, and C16:2 were observed in increasingly lower abundance. In very low abundance were C18:0, C18:1, C14:0, C24:0, and heptadecane. In addition to the fatty acids identified, several phytol tails were identified in the FAME trace through GC-MS. Following 3 days of increasingly nitrogen deplete culturing, higher relative ratios of saturated fatty acids were observed, as shown in Fig. 3B. The most abundant FAME was C16:0, with all other FAMEs in much lower comparative abundance. Despite the overall shift towards C16:0, several unsaturated C18 FAMES, C18:2 and C18:1, showed relative increases. C13:0 was used as an internal standard in these runs and was not a FAME produced by *P. celeri*.

Using an Agilent J&W GC Column DB-Wax column, the location of unsaturation and quantification of the six most abundant FAMEs were identified throughout gradual nitrogen restriction, as shown in Fig. 3C. The percentage of C18:3n3 and C16:3 decreased from day 0 to day 3 of nitrogen restriction, while C16:0 increased. Uniquely compared to other unsaturated FAMEs, the relative percentages of C18:2n6 and C18:1n9 increased during nitrogen restriction. When quantified using GC-FID, the six most abundant FAMEs identified in Fig. 3C accounted for more than 80% of total FAMEs.

3.3. Carbohydrates and monosaccharides

Total carbohydrate analysis using anthrone revealed a significant increase in carbohydrate content as a result of gradual nitrogen deprivation (Fig. 2B). Monosaccharide analysis showed the relative carbohydrate composition, as shown in Fig. 4A. Under nutrient-replete conditions, *P. celeri* had large fractions of glucose (25 ± 8%), mannose (37 ± 4%), and galactose (28 ± 3%), with a small relative percentage of ribose (8 ± 1%) and less than 2% of total monosaccharides identified as rhamnose and xylose. Nitrogen deprivation resulted in a substantial increase in the relative levels of glucose, which represented nearly 80% of the total carbohydrates on days 2 and 3. The four primary monosaccharides (glucose, mannose, galactose and ribose) accounted for over 90% of the total carbohydrates throughout nitrogen deprivation.

Enzymatic starch quantification using the Sigma-Aldrich Starch Assay Kit showed an average of 61 ± 3% starch per AFDW in triplicate nitrogen deplete samples (2 replicates at 40 ppm N, 1 replicate from day 2 of gradual nitrogen restriction) with an average of 53 ± 5% total carbohydrate per AFDW reported from anthrone. Therefore, enzymatic total starch analysis agreed closely with anthrone total carbohydrate values. As shown in Fig. 4B, transmission electron microscopy (TEM) imaging of *P. celeri* biomass at the end of 3 days of gradual nitrogen deprivation revealed large starch granules throughout the *P. celeri* chloroplast. TEM imaging of 40 ppm N restricted cells had similar starch granules (Fig. 4C), consistent with the high levels of carbohydrate quantified biochemically.

To evaluate the metabolic potential for starch production, starch synthesis genes in the well-characterized green alga *Chlamydomonas reinhardtii* were compared to potential homologs in *P. celeri* using BLAST (Deschamps et al., 2023). *C. reinhardtii* has been shown to produce high-starch biomass under nutrient depletion, and thus was chosen for comparison to *P. celeri* (Work et al., 2010). Inside the chloroplast of *C. reinhardtii*, several enzymes form a pathway to convert fructose-6-phosphate from the Calvin Benson Bassham cycle to ADP-glucose, and ultimately starch. As shown in Table 1, genes for the enzymes PGI, PGM, and AGPase (a hetero-tetramer encoded by *Sta1* and *Sta6*), were identified in *P. celeri* with high (>70%) similarity to those found in *C. reinhardtii*. Genes involved in the synthesis of amylopectin (both from ADP-glucose and other starch precursors) were identified in *P. celeri*, with nearly 70% similarity to orthogonal genes in *C. reinhardtii*. These included both starch synthases, *SS1*, *SS2*, *SS3*, and *SS4*, as well as trans-glycosidases, *ISA1* and *ISA2*. Genes encoding starch branching enzymes, BE1, BE2, and BE3, were also identified in *P. celeri* with high similarity to *C. reinhardtii*.

3.4. Proteins and amino acids

The amino acid composition of nutrient-replete *P. celeri* biomass, with 51 ± 10% (reported from Lowry) total protein per AFDW (Fig. 2A), was compared to day 3 nitrogen deplete and 2X sea salt biomass to evaluate relative changes, as shown in Fig. 5. For all three conditions, most of the amino acid ratios remained similar, with all three conditions containing the 9 essential amino acids. In all three conditions, His, Cys, Trp, and Met were present at very low levels. A significant increase in the relative levels of Pro was observed under 2X sea salt, with this amino acid representing nearly 20% of the amino acids detected. Total protein data derived from the Lowry assay was similar to total protein derived from AAA. Total protein for increasingly deplete (Fig. 2B), and 2X sea salt (Fig. 2D) are reported from AAA, and total protein for nutrient-replete (Fig. 2A), 40 ppm N (Fig. 2C) is reported from Lowry.

4. Discussion

4.1. Proximate composition of Picochlorum celeri

Picochlorum is of high interest for industrial microalgal cultivation, exhibiting some of the highest outdoor productivities reported to date. Over the past few years, several *Picochlorum* species and strains have been investigated to better understand how these microalgae might be useful in the production of renewable commodities (Barten et al., 2020; Dahlin et al., 2019; de la Vega et al., 2011; Franks et al., 2022; Krishnan et al., 2021; Weissman et al., 2018). *Picochlorum celeri* TG2 is noteworthy because of its productive outdoor growth, high light tolerance, and available methods of genetic engineering for potential strain improvements (Krishnan et al., 2020; Weissman et al., 2018). However, detailed biomass characterization of *P. celeri* TG2 was not previously published. Quantification of the carbohydrate, protein, fatty acid, pigment, and nucleotide components in *P. celeri* biomass under varying conditions provides direction in cultivation and harvesting approaches towards maximal flux such that the most valuable biomass components can be generated (Barbosa et al., 2023).

In this study, the carbohydrate, protein, fatty acid, chlorophyll, and nucleotide contents of *P. celeri* were measured in nutrient dense sea salt media under nutrient-replete, increasingly nitrogen depleted, 40 ppm N, and hyper saline (2X sea salt) conditions to understand the relative biomass partitioning as a result of changes in nutrient levels. Multiple orthogonal analytical methods including anthrone total carbohydrate analysis and monosaccharide analysis, as well as Lowry total protein analysis and amino acid analysis (AAA), were employed to quantify a shift from protein-rich biomass to carbohydrate-rich biomass in both gradual nitrogen depletion as well as 40 ppm N restriction. A shift towards a cellular storage product (carbohydrates/starch) is commonly observed for microalgae (Newell Arber, 1901) and has been recently documented in *Picochlorum renovo* (Dahlin et al., 2019). In many prior studies, a shift towards carbohydrate-rich biomass was achieved through batch-growth nutrient exhaustion (Dahlin et al., 2018, 2019).

Here, a carbohydrate increase was achieved through both gradual nitrogen depletion as well as repeated daily addition of a medium containing 40 ppm N. Gradual nitrogen depletion revealed that the shift from protein towards carbohydrate storage products took several days due to the large excess N content (200 ppm) used in the nutrient-replete sea salt media reported here. Once nitrogen depletion was achieved on day 3, biomass productivity was near zero, as shown in Fig. 2B. To induce a shift from protein-rich to carbohydrate-rich biomass without severe productivity declines, sea salt media containing 40 ppm N was used. The 40 ppm N experiment resulted in high productivity (36 ± 0.4 g AFDW m^{-2} day^{-1}) along with carbohydrate-rich (54 ± 9% AFDW) biomass. These data highlight an attractive, pond-relevant approach

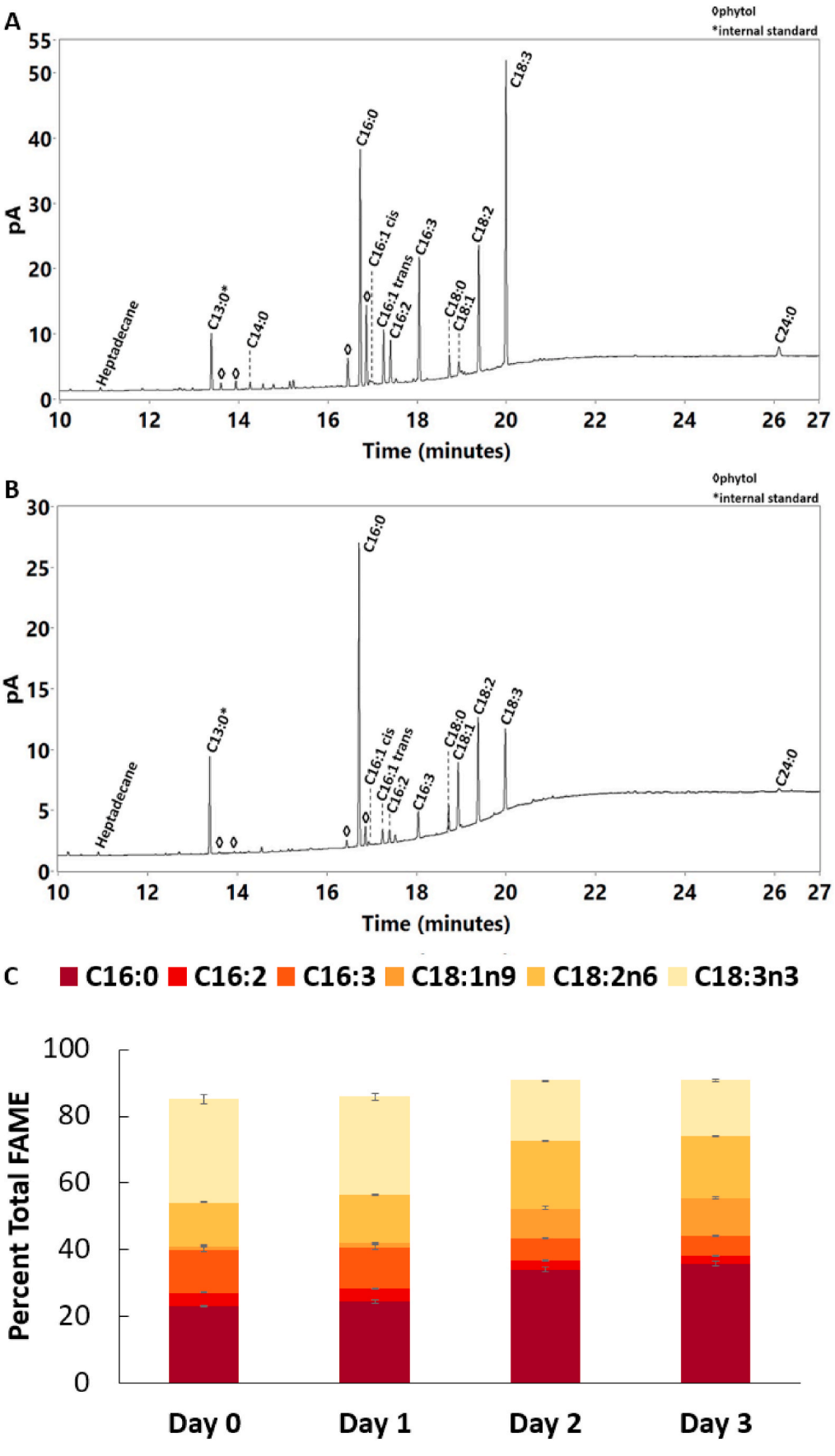

(caption on next page)

Fig. 3. A. GC-FID chromatogram of identified fatty acid methyl ester (FAME) composition of *Picochlorum celeri* biomass on day 3 when grown under nutrient-replete conditions in sea salt media in a bioreactor at 33 °C using diel lighting with a 60% volumetric dilution after sunset. **B.** GC-FID chromatogram of identified fatty acid methyl ester (FAME) composition of *Picochlorum celeri* biomass on day 3 of nitrogen-deplete growth conditions in sea salt media in a bioreactor at 33 °C using diel lighting with a 60% volumetric dilution in N-free sea salt media after sunset. **C.** Identified FAME composition in *Picochlorum celeri* under nutrient-replete (day 0) and increasingly nitrogen deplete (days 1–3) sea salt media grown in biological triplicate in a bioreactor at 33 °C using diel lighting with a 60% volumetric dilution after sunset for 3 days.

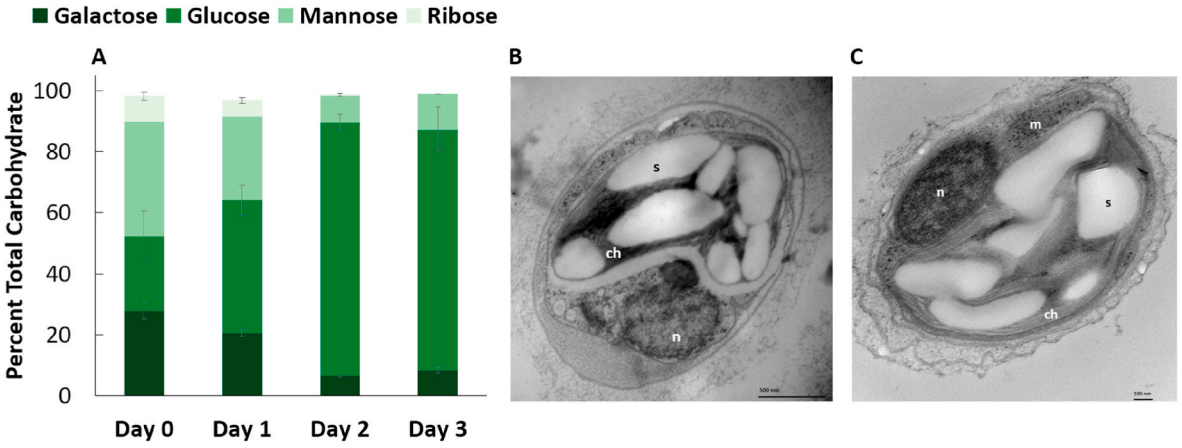

Fig. 4. A. Average identified monosaccharide composition of *Picochlorum celeri* biomass under nutrient-replete (day 0) and increasingly nitrogen deplete (days 1–3) sea salt media cultivation in biological triplicate in a bioreactor at 33 °C using diel lighting with a 60% volumetric dilution after sunset for 3 days. **B.** Transmission electron microscopy (TEM) image of starch-rich *Picochlorum celeri* following 3 days of 60% volumetric dilutions in nitrogen-free sea salt media grown in a bioreactor at 33 °C using diel lighting with the nucleus (n), chloroplast (ch), and starch (s) indicated. **C.** Transmission electron microscopy (TEM) image of starch-rich *Picochlorum celeri* in 40 ppm N sea salt media grown in a bioreactor at 33 °C using diel lighting with a 60% volumetric dilution 1 h prior to sunset with the nucleus (n), mitochondria (m), chloroplast (ch), and starch (s) indicated.

(restricted nitrogen cultivation) to attain high levels of carbohydrates without suffering large productivity penalties, and are consistent with previously reported semi-continuous nitrogen restriction in *Chaetoceros* sp. (Weissman and Goebel, 1987).

4.2. Comparison to Picochlorum renovo and Scenedesmus sp. NREL46B-D3

Nutrient stress, including nitrogen limitation and hyper-saline conditions, in microalgae and cyanobacteria has been widely studied for decades, with documented changes in biomass composition within an organism as well as species distribution within an ecosystem (Dignum et al., 2005). As documented in Dahlin et al. (2019), the proximate composition of closely related *Picochlorum renovo* was well characterized under batch growth conditions (Dahlin et al., 2019). Like *P. celeri*, *P. renovo* biomass consisted mainly of protein under nutrient-replete conditions. Likewise, this biomass shifted towards carbohydrates (mainly the starch monomer glucose) under batch culturing wherein cell growth led to nitrogen-deplete conditions. Both *P. celeri* and *P. renovo* show significant galactose, mannose, and ribose fractions under nutrient-replete conditions. Under nitrogen deplete conditions, total carbohydrates are instead dominated by glucose as the primary hydrolysis monomer, in both organisms. Throughout nutrient-replete and deplete cultivation, *P. celeri* and *P. renovo* contain 10–15% FAME/AFDW. However, *P. celeri* contains larger proportions of C16:2 (~3.2% of total FAMEs) in comparison to *P. renovo* (~1.2% of total FAMEs, Dr. Lukas Dahlin, personal communication). Finally, while the Dahlin et al. (2019) study in *P. renovo* produced high-carbohydrate biomass through batch growth, it is unclear if this phenotype could be maintained in a mass cultivation-relevant regime of daily harvests and dilutions, as performed in this study. Our data highlight the fact that *P. celeri* can produce high-carbohydrate biomass while maintaining high productivity via daily harvests and dilutions in nitrogen-restricted 40 ppm N media.

Published work from Calhoun et al. (2021) reported biomass compositional analysis data for *Scenedesmus* sp. *NREL 46B-D3* (Calhoun et al., 2021). This *Scenedesmus*, like *Picochlorum* spp., is a halotolerant green microalga, with a fast growth rate and potential industrial cultivation applications. *Scenedesmus* sp. *NREL 46B-D3* showed an increase in carbohydrates during nitrogen limited batch cultivation. This was indicative of high starch biomass, like that reported for *P. celeri* in this manuscript. Interestingly, *Scenedesmus* sp. *NREL 46B-D3* showed a simultaneous increase in lipid content along with the aforementioned carbohydrates. This increase is unique compared to *Picochlorum* spp. and suggests that *Scenedesmus* sp. *NREL 46B-D3* uses both lipids and carbohydrates for cellular storage, unlike *Picochlorum* spp. which mainly exhibit carbohydrate increases during nitrogen depletion.

4.3. Carbohydrates, starch, and monosaccharides

Based on the published biomass composition of other strains of *Picochlorum*, it was hypothesized that the primary storage carbohydrate in *P. celeri* was the glucose polymer starch (Dahlin et al., 2019). Monosaccharide data showing an increase in glucose following nitrogen depletion or restriction supports this hypothesis. Genome analysis identified 15 homologous starch synthesis genes in *P. celeri* when compared to *C. reinhardtii*. Furthermore, a TEM image of *P. celeri* following 3 days of gradual nitrogen restriction showed the presence of multiple large granules. Finally, a direct measurement of starch content using enzymatic digestion (a-1,4 and a-1,6 glucose hydrolysis by amyloglucosidase) showed >50% starch content in high-carbohydrate, nitrogen-restricted biomass. These data are consistent with the production of starch as the primary cellular storage product in *P. celeri*. Although expected, it was important to biochemically verify that starch was the cellular glucose store.

Microalgal starch is of industrial interest because it can be used in the synthesis of bioplastics as well as a suite of fuel and platform chemical intermediates using conventional fermentative technologies. Using

Table 1
BLAST comparison of starch synthesis genes from *Chlamydomonas reinhardtii* and *Picochlorum celeri* with genes identified using Geneious grade (*combines query coverage, e-value, and identity values for each hit with weights 0.5, 0.25 and 0.25) and identical genes highlighted within each group.

C. reinhardtii			*P. celeri*	
Gene	***Phytozome Reference***	***Function***	***Grade* from BLAST***	***Gene Annotation (identified with >50% grade)***
PGI	Cre03.g175400	Fructose-6-Phosphate to Glucose-6-Phosphate	74.5%	Glucose-6-phosphate isomerase, cytosolic 1
			77.8%	Glucose-6-phosphate isomerase like protein| domain 1
PGM	Cre06.g278210	Glucose-6-Phosphate to Glucose-1-Phosphate	83.0%	Phosphoglucomutase, first 3 domains
STA1	Cre13.g567950	Glucose-1-Phosphate to ADP-Glucose	79.4%	Glucose-1-phosphate adenylyltransferase
			73.4%	Glucose-1-phosphate adenylyltransferase small subunit, chloroplastic/amyloplastic
			68.5%	Glucose-1-phosphate adenylyltransferase small subunit
			67.2%	Glucose-1-phosphate adenylyltransferase small subunit, chloroplastic/amyloplastic
STA6	Cre03.g188250	Glucose-1-Phosphate to ADP-Glucose	81.0%	Glucose-1-phosphate adenylyltransferase small subunit
			74.0%	Glucose-1-phosphate adenylyltransferase
			67.8%	Glucose-1-phosphate adenylyltransferase small subunit, chloroplastic/amyloplastic
			67.5%	Glucose-1-phosphate adenylyltransferase small subunit, chloroplastic/amyloplastic
AGP2	Cre16.g683450	Glucose-1-Phosphate to ADP-Glucose	69.7%	Glucose-1-phosphate adenylyltransferase
			68.4%	Glucose-1-phosphate adenylyltransferase small subunit
AGP3	Cre07.g331300	Glucose-1-Phosphate to ADP-Glucose	54.7%	Glucose-1-phosphate adenylyltransferase
			53.9%	Glucose-1-phosphate adenylyltransferase small subunit, chloroplastic/amyloplastic
			52.1%	Glucose-1-phosphate adenylyltransferase small subunit
SS1	Cre04.g215150	Starch precursor to (amylopectin)	69.1%	Starch synthase, chloroplastic/amyloplastic
			67.7%	Soluble starch synthase 3, chloroplastic/amyloplastic
			67.2%	Starch synthase, chloroplastic/amyloplastic
			66.6%	Starch synthase, chloroplastic/amyloplastic
			56.2%	Starch synthase, chloroplastic/amyloplastic
			51.2%	Soluble starch synthase 3, chloroplastic/amyloplastic
SS2	Cre03.g185250	Starch precursor to (amylopectin)	70.9%	Starch synthase, chloroplastic/amyloplastic
			61.0%	Starch synthase, chloroplastic/amyloplastic
			60.8%	Soluble starch synthase 3, chloroplastic/amyloplastic
			60.1%	Starch synthase, chloroplastic/amyloplastic
			59.9%	Starch synthase, chloroplastic/amyloplastic
			59.8%	Soluble starch synthase 3, chloroplastic/amyloplastic
SS3	Cre13.g579598	ADP-Glucose to starch (amylopectin)	79.3%	Soluble starch synthase 3, chloroplastic/amyloplastic
			77.3%	Soluble starch synthase 3, chloroplastic/amyloplastic
			74.6%	Starch synthase, chloroplastic/amyloplastic
			73.6%	Starch synthase, chloroplastic/amyloplastic
			65.9%	Starch synthase, chloroplastic/amyloplastic
			58.4%	Starch synthase, chloroplastic/amyloplastic
SS4	Cre16.g665800	ADP-Glucose to starch (amylopectin)	74.5%	Starch synthase, chloroplastic/amyloplastic
			64.8%	Soluble starch synthase 3, chloroplastic/amyloplastic
			63.8%	Starch synthase, chloroplastic/amyloplastic
			63.7%	Starch synthase, chloroplastic/amyloplastic
			63.6%	Soluble starch synthase 3, chloroplastic/amyloplastic
			50.9%	Starch synthase, chloroplastic/amyloplastic
BE1	Cre06.g289850	Starch branching enzyme	76.7%	(Trans)glycosidases
			71.5%	1,4-alpha-glucan branching enzyme II
BE2	Cre06.g270100	Starch branching enzyme	83.2%	1,4-alpha-glucan branching enzyme II
			66.2%	(Trans)glycosidases
BE3	Cre10.g444700	Starch branching enzyme	83.0%	1,4-alpha-glucan branching enzyme II
			65.7%	(Trans)glycosidases
ISA1	Cre03.g155001	Starch precursor to amylopectin	65.5%	(Trans)glycosidases
			59.0%	(Trans)glycosidases
ISA2	Cre17.g698850	Starch precursor to amylopectin	63.7%	(Trans)glycosidases
			58.6%	(Trans)glycosidases
			57.0%	(Trans)glycosidases

more traditional fermentation methods, microalgal glucose can be converted to bioethanol for sustainable fuel and aviation applications. *Saccharomyces cerevisiae* fermentation of microalgal glucose followed by distillation resulted in 95% pure bioethanol (Rony et al., 2023). Ethanol is under high worldwide demand as a fuel additive, with the United States and Brazil producing >100 billion L per year from primarily corn and sugarcane. Such crops have high fresh water and land use requirements, and compete with food production resulting in increased food cost (Mohapatra et al., 2018). Therefore, high productivity marine microalgae, like *P. celeri*, with a high carbohydrate yield following 40 ppm N dilutions is a compelling alternate source of biofuels via fermentation.

Algal starch has been used directly in the production of bioplastics, with a study from Mathiot et al. (2019) describing the direct plasticization of *C. reinhardtii* biomass containing 49% starch with glycerol in a twin-screw extruder (Mathiot et al., 2019). Thermo-plastic processing of up to 30% starch followed by heat and pressure treatment resulted in the production of a highly elastic, transparent bioplastics with similar optical and tensile properties to its non-biodegradable competitor. This renewable material could replace traditional oil-based packaging materials (Gonzalez-Gutierrez et al., 2010). Monomeric glucose has its own industrial utility, as documented in the production of non-isocyanate polyurethane rigid foams from glucose with dimethyl carbonate and hexamethylene diamine (Xi et al., 2019). Poor-recycling and significant plastic waste from traditional plastics make bioplastics a compelling solution to the increasing global demand for plastic products. Microalgae, including *P. celeri*, may provide a useful renewable platform to produce bioplastic precursors including starch (Chia et al., 2020).

While the glucose polymer starch was the primary storage product observed under nitrogen-deplete and limited conditions, under nutrient-replete conditions other monomeric sugars were also detected (e.g., galactose, mannose, ribose), indicating the possible presence of additional carbohydrate polymers of interest. Galactomannans are industrially-relevant biopolymers consisting of a mannose backbone

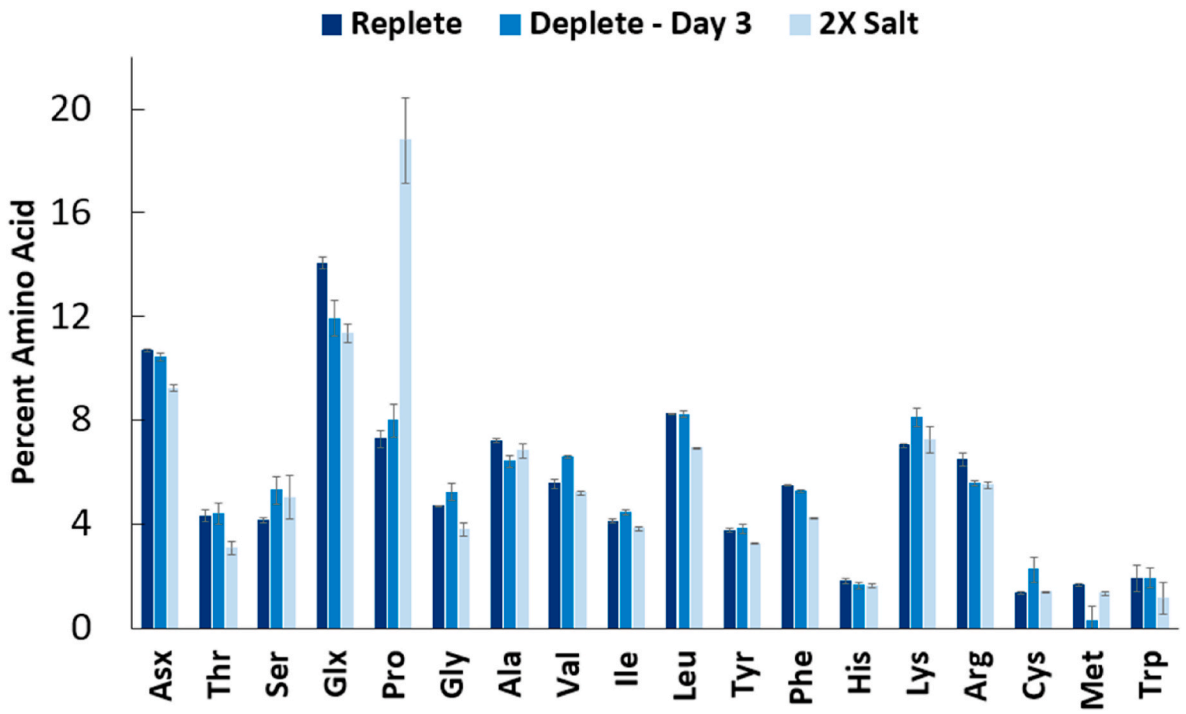

Fig. 5. Average identified amino acid composition of *Picochlorum celeri* biomass grown in nutrient-replete (day 3), nitrogen-deplete (day 3; biological triplicate), and hyper-saline (2X sea salt; 80 ppt) media (days 2 and 3; biological duplicate) in a bioreactor at 33 °C using diel lighting with a 60% volumetric dilution after sunset for 3 days.

with galactose side chains. Higher plants provide the primary source of commercial galactomannans including locust bean gum (*Ceretonia siliqua*), guar gum (*Cyamopsis tetragonolobus*), and fenugreek (*Trigonella*), with unique mannose:galactose ratios resulting in the differing properties of each (Thombare et al., 2016; Wu et al., 2012). Given the presence of 28 ± 3% galactose and 37 ± 4% mannose in the carbohydrate fraction of nutrient-replete *P. celeri*, it is reasonable to hypothesize some presence of galactomannans and future work in this area would be beneficial to quantify such biopolymers. Furthermore, mannose- and galactose-containing biomass could provide a renewable source of monosaccharides for the development of synthetic galactomannans.

4.4. Proteins and amino acids

In nutrient-replete media, a majority of quantified *P. celeri* biomass was protein. High protein microalgae are of interest in commercial production as a nutritional supplement (Gautam et al., 2021). Proteins play an essential role in both human and animal feed as the major building block for muscle tissue. Plant-based protein supplements may contain limited essential amino acids, requiring the inclusion of several plant-based protein sources to balance the amino acid profile in a vegan supplement. For example, pea protein is limited in its methionine content (Met, 0.5% total protein), while soy protein is limited in valine content (Val, 3.5% total protein). AAA data showed that *P. celeri* contained all 9 essential amino acids under nutrient-replete conditions, including methionine (Met, 1.7% total protein) and valine (Val, 5.5% total protein). Whey, the commercial standard, shows similar levels of Met (2.2% total protein) and Val (4.2% total protein) (Gorissen et al., 2018). The presence of these two amino acids, as well as the other six essential amino acids, makes *P. celeri* a compelling vegan protein source when compared to pea or soy.

When considering the possibilities of *P. celeri* as a nutritional supplement platform, nucleotide levels must be taken into consideration. While some nucleotides can be beneficial in human nutritional supplements and animal feed, high levels of nucleotides can become detrimental. In juvenile gilthead sea bream, supplementation of yeast containing 6% RNA enhanced growth and provided adequate nitrogen supplementation. However, RNA concentrations above 6% were harmful to fish growth (Huu, 2016). Similar issues were observed when using microbial biomass as a human food source, with subjects showing high plasma and urinary uric acid concentrations following the consumption of a yeast (*Torulopsis utilis*, 11.4% nucleic acids), indicative of the development of gout (Waslien et al., 1970). *Picochlorum celeri* under nutrient-replete conditions contained 5.7 ± 1% nucleotides, ~90% of which was RNA. In sum, these data suggest that *P. celeri* could be an appropriate feed platform.

Under 2X sea salt conditions, AAA results revealed an interesting biological mechanism for salt tolerance. Proline (Pro) comprised nearly 20% of the total amino acids in 2X sea salt media. These data suggest that Pro may play a role as an osmolyte in *P. celeri*. Many microalgae and cyanobacteria utilize small molecular weight, neutrally charged molecules including amino acids, to maintain osmotic balance (Zea Obando et al., 2016). While both Pro and glycerol have been proposed as osmolytes for other species of *Picochlorum* this is the first time an osmolyte under hypersaline conditions has been directly detected and quantified for *Picochlorum celeri* (Foflonker et al., 2018).

4.5. Lipids and FAMEs

Several useful industrial products can be derived from microalgal fatty acids, most notably biofuels, including sustainable aviation fuels (SAFs) (Wijffels and Barbosa, 2010). For commercial biodiesel, fatty acids between C16 and C18 in length are most common (Suastes-Rivas et al., 2020). While several FAME properties influence biodiesel performance, low temperature performance and oxidative stability are of primary concern. A low relative concentration of long-chain saturated FAMEs prevents cold temperature wax formation. Oxidative stability is improved by higher relative concentrations of saturated and monounsaturated FAMEs, and lower concentrations of polyunsaturated FAMEs (Hoekman et al., 2012). *Picochlorum celeri* shows low

concentrations of polyunsaturated FAMEs under both nutrient-replete and deplete conditions. The shift in FAME content towards C16:0 under nitrogen restriction may prove useful in improving the cold temperature performance of *P. celeri* derived biodiesel. Likewise, with *P. celeri* containing around 11% FAME per AFDW under nutrient-replete, 40 ppm N restricted, and 3-day nitrogen depleted conditions, there is no relative biomass partitioning penalty for a low-nitrogen culturing strategy to obtain higher relative C16:0. Furthermore, the presence of heptadecane is useful from a fuel perspective, as alkanes are a direct drop-in fuel. While the relative percentage of heptadecane is very small, when considered on a commercial scale, a degree of useable heptadecane may be obtained from industrial *P. celeri* production for biofuels. Additionally, algal fatty acids can be a source of value-added products including polyurethane precursors. Palmitoleic acid (C16:1 cis) can be used as a starting point for renewable polyurethane production (Phung Hai et al., 2020). Nutrient-replete *P. celeri* biomass contains a degree of palmitoleic acid, and other saturated fatty acids, making *P. celeri* lipids a potential source for both renewable fuels and biopolymers.

4.6. Chlorophylls and pigments

Photosynthetic organisms use chlorophylls for light harvesting, with green algae composed primarily of chlorophyll *a and b*. With its vibrant green color, chlorophyll has been used for nearly a century as a natural food coloring agent and proposed naturopathic supplement (Schertz, 1927). In *P. celeri*, chlorophyll is 4.4 ± 0.2% AFDW under nutrient-replete (200 ppm N) conditions, with a significant decline observed under gradual nitrogen depletion. This is expected as the algae divert cellular metabolism towards carbohydrate production and away from nitrogen-rich macromolecules. During 40 ppm N restricted growth, chlorophyll decreases by half to 2.1 ± 0.3% AFDW (Weissman et al., 2018). In addition to chlorophylls, microalgae contain a variety of other light harvesting pigments. Prior work from Cano et al. (2021) details the total pigment composition of *P. celeri* under varying light conditions. Fast-growing, nutrient-replete *P. celeri* had a pigment content of ~6.5% AFDW under the diel conditions used, including a significant proportion of lutein (~10% total pigments), with increasingly smaller relative proportions of β-carotene, neoxanthin, violaxanthin, canthaxanthin, and zeaxanthin under both high and low light acclimation states (Cano et al., 2021). Commercially, microalgal pigments are of interest for their prophylactic benefits. High dietary pigment consumption can have antioxidant, anti-inflammatory, and anti-carcinogenic benefits (Patel et al., 2022). Lutein specifically has been reported to improve vision problems including macular degeneration and cataracts, and had neuroprotective and anti-inflammatory effects when consumed over time (Mitra et al., 2021). With high lutein levels in nutrient-replete *P. celeri* biomass, cultivation for high value nutraceuticals may improve the techno-economic viability of this microalgae.

Under nutrient-replete, increasingly nitrogen depleted, 40 ppm N, and 2X sea salt conditions, *P. celeri* biomass was characterized with less than 30% unknown biomass remaining under all conditions. It is postulated that the majority of unidentified biomass was small polar metabolites, vitamins or carotenoids, or additional major metabolites (carbohydrates, lipids, proteins) that were not detected during analysis (Van Wychen et al., 2021). Additional methods of biomass fractionation could be employed in the future to better resolve the unknown biomass that remains in this study (Van Wychen et al., 2021).

5. Conclusions

For this study, a detailed biomass proximate characterization of *P. celeri* was conducted to characterize the biomass partitioning of this organism under nutrient-replete, nitrogen-restricted (daily 60% volumetric dilutions in 40 ppm N-containing medium), nitrogen deplete (3 days of 60% volumetric dilutions in N-free medium), and 2X sea salt (40 ppm Instant Ocean) conditions. These data demonstrate how *P. celeri* biomass shifted as a result of nitrogen restriction (from high protein to high carbohydrate) and suggests a pond-relevant 40 ppm N-limited cultivation strategy to produce high carbohydrate *P. celeri* biomass without significant productivity compromises. Under high-salt conditions, the biomass composition was similar to nutrient-replete, however AAA revealed a significant increase in the relative level of Pro, suggesting that this functions as an osmolyte in *P. celeri*. This detailed characterization of *P. celeri* biomass provides a roadmap for how this fast-growing microalga might be used in the production of useful commodities including bioplastics, polyurethanes, nutritional supplements, and biofuels including SAFs.

Declaration of authors agreement to authorship and submission

All authors have agreed to authorship and the submission of this manuscript for peer review.

CRediT authorship contribution statement

Alaina J. LaPanse: Conceptualization, Data curation, Formal analysis, Investigation, Methodology, Validation, Visualization, Writing – original draft, Writing – review & editing. **Anagha Krishnan:** Data curation, Formal analysis, Investigation, Methodology, Validation, Writing – review & editing. **Galen Dennis:** Data curation, Validation, Visualization, Writing – review & editing. **Devin A.J. Karns:** Methodology, Resources, Software, Writing – review & editing. **Lukas R. Dahlin:** Conceptualization, Formal analysis, Project administration, Validation, Writing – review & editing. **Stefanie Van Wychen:** Data curation, Writing – review & editing. **Tyson A. Burch:** Conceptualization, Formal analysis, Writing – review & editing. **Michael T. Guarnieri:** Formal analysis, Funding acquisition, Project administration, Resources, Supervision, Writing – review & editing. **Joseph C. Weissman:** Conceptualization, Formal analysis, Project administration, Supervision, Writing – review & editing. **Matthew C. Posewitz:** Conceptualization, Formal analysis, Funding acquisition, Project administration, Resources, Supervision, Validation, Writing – original draft, Writing – review & editing.

Declaration of competing interest

The authors declare that they have no known competing financial interests or personal relationships that could have appeared to influence the work reported in this paper.

Data availability

Data will be made available on request.

Acknowledgements

This work was financially supported by the Department of Energy, Office of Energy Efficiency and Renewable Energy (EERE), Algae Biotechnology Partnership, under Agreement No. 28812. This work was co-authored by the National Renewable Energy Laboratory, operated by Alliance for Sustainable Energy, LLC, for the U.S. Department of Energy (DOE) under Contract No. DE-AC36-08GO28308. The views expressed in the article do not necessarily represent the views of the DOE or the U. S. Government. The U.S. Government retains and the publisher, by accepting the article for publication, acknowledges that the U.S. Government retains a nonexclusive, paid-up, irrevocable, worldwide license to publish or reproduce the published form of this work, or allow others to do so, for U.S. Government purposes.

We thank John Schulze at the Molecular Structure Facility (part of the Genome Center at the University of California, Davis) for performing the Amino Acid Analysis.

We thank the Boulder EM Services Core Facility (MCDB Department

at the University of Colorado, Boulder) for electron microscopy sample preparation and imaging, with the technical assistance of Garry P. Morgan and Sarah Ann Zimmermann in particular.

Appendix A. Supplementary data

Supplementary data to this article can be found online at https://doi.org/10.1016/j.plaphy.2024.108364.

References

Barbosa, M.J., Janssen, M., Südfeld, C., D'Adamo, S., Wijffels, R.H., 2023. Hypes, hopes, and the way forward for microalgal biotechnology. Trends Biotechnol. 41, 452–471. https://doi.org/10.1016/j.tibtech.2022.12.017.

Barten, R.J.P., Wijffels, R.H., Barbosa, M.J., 2020. Bioprospecting and characterization of temperature tolerant microalgae from Bonaire. Algal Res. 50 https://doi.org/10.1016/j.algal.2020.102008.

Becker, S.A., Spreafico, R., Kit, J.L., Brown, R., Likhogrud, M., Fang, W., Posewitz, M.C., Weissman, J.C., Radakovits, R., 2020. Phased diploid genome sequence for the fast-growing microalga *Picochlorum celeri*. Microbiol Resour Announc 9, 14–16. https://doi.org/10.1128/mra.00087-20.

Breuer, G., Lamers, P.P., Martens, D.E., Draaisma, R.B., Wijffels, R.H., 2012. The impact of nitrogen starvation on the dynamics of triacylglycerol accumulation in nine microalgae strains. Bioresour. Technol. 124, 217–226. https://doi.org/10.1016/j.biortech.2012.08.003.

Calhoun, S., Bell, T.A.S., Dahlin, L.R., Kunde, Y., LaButti, K., Louie, K.B., Kuftin, A., Treen, D., Dilworth, D., Mihaltcheva, S., Daum, C., Bowen, B.P., Northen, T.R., Guarnieri, M.T., Starkenburg, S.R., Grigoriev, I.V., 2021. A multi-omic characterization of temperature stress in a halotolerant *Scenedesmus* strain for algal biotechnology. Commun. Biol. 4 https://doi.org/10.1038/s42003-021-01859-y.

Cano, M., Karns, D.A.J., Weissman, J.C., Heinnickel, M.L., Posewitz, M.C., 2021. Pigment modulation in response to irradiance intensity in the fast-growing alga *Picochlorum celeri*. Algal Res. 58 https://doi.org/10.1016/j.algal.2021.102370.

Chia, W.Y., Ying Tang, D.Y., Khoo, K.S., Kay Lup, A.N., Chew, K.W., 2020. Nature's fight against plastic pollution: algae for plastic biodegradation and bioplastics production. Environ. Sci. Ecotechnol. 4 https://doi.org/10.1016/j.ese.2020.100065.

Chomczynski, P., Sacchi, N., 1987. Single-step method of RNA isolation by acid guanidinium thiocyanate-phenol-chloroform extraction. Anal. Biochem. 162, 156–159.

Cooper, C., Packer, N., Williams, K., 2000. Amino acid analysis protocols. Methods in Molecular Biology. Humana Press, Totawa.

Dahlin, L.R., Gerritsen, A.T., Henard, C.A., Kunde, Y., Hovde, B.T., Starkenburg, S.R., Wychen, S. Van, Linger, J.G., Posewitz, M.C., Guarnieri, M.T., 2019. Development of a high-productivity, halophilic, thermotolerant microalga *Picochlorum renovo*. Commun. Biol. 1 https://doi.org/10.1038/s42003-019-0620-2. –9.

Dahlin, L.R., Guarnieri, M.T., 2022. Heterologous expression of phosphite dehydrogenase in the chloroplast or nucleus enables phosphite utilization and genetic selection in *Picochlorum spp*. Algal Res. 62 https://doi.org/10.1016/j.algal.2021.102604.

Dahlin, L.R., Guarnieri, M.T., 2021. Development of the high-productivity marine microalga , *Picochlorum renovo* , as a photosynthetic protein secretion platform. Algal Res. 54, 102197 https://doi.org/10.1016/j.algal.2021.102197.

Dahlin, L.R., Van Wychen, S., Gerken, H.G., McGowen, J., Pienkos, P.T., Posewitz, M.C., Guarnieri, M.T., 2018. Down-selection and outdoor evaluation of novel, halotolerant algal strains for winter cultivation. Front. Plant Sci. 871 https://doi.org/10.3389/fpls.2018.01513.

de la Vega, M., Díaz, E., Vila, M., León, R., 2011. Isolation of a new strain of *Picochlorum sp* and characterization of its potential biotechnological applications. Biotechnol. Prog. 27, 1535–1543. https://doi.org/10.1002/btpr.686.

Deschamps, P., Ball, S.G., Dauvillee, D., 2023. The comparative, biochemistry, genetics, and evolution of starch metabolism in *Chlamydomonas reinhardtii*. In: Grossman, A. R., Wollman, F.-A. (Eds.), The Chlamydomonas Sourcebook. Elsevier, pp. 23–44.

Dignum, M., Matthijs, H.C.P., Pel, R., Laanbroek, H.J., Mur, L.R., 2005. Nutrient limitation of freshwater cyanobacteria. In: Harmful Cyanobacteria, pp. 65–86.

Dolezel, J., Bartos, J., Voglmayr, H., Greilhuber, J., 2003. Nuclear DNA content and genome size of trout and human. Cytometry 51A, 127–128. https://doi.org/10.1002/cyto.a.10013.

Dreywood, R., 1946. Qualitative test for carbohydrate. Material. Indust. Eng. Chem. - Anal. Edit. 18, 499. https://doi.org/10.1021/i560156a015.

Fawzy, S., Osman, A.I., Doran, J., Rooney, D.W., 2020. Strategies for mitigation of climate change : a review intergovernmental panel on climate change. Environ. Chem. Lett. 18, 2069–2094. https://doi.org/10.1007/s10311-020-01059-w.

Finkel, Z.V., Follows, M.J., Liefer, J.D., Brown, C.M., Benner, I., Irwin, A.J., 2016. Phylogenetic diversity in the macromolecular composition of microalgae. PLoS One 11. https://doi.org/10.1371/journal.pone.0155977.

Foflonker, F., Mollegard, D., Ong, M., Yoon, H.S., Bhattacharya, D., 2018. Genomic analysis of *Picochlorum* species reveals how microalgae may adapt to variable environments. Mol. Biol. Evol. 35, 2702–2711. https://doi.org/10.1093/molbev/msy167.

Foley, P.M., Beach, E.S., Zimmerman, J.B., 2011. Algae as a source of renewable chemicals: opportunities and challenges. Green Chem. 13, 1399–1405. https://doi.org/10.1039/c1gc00015b.

Franks, D.T., Sabella, T.J., Henley, W.J., 2022. Minimum nitrogen cell quota for maximal growth rate in cycloturbidostat cultures of *Picochlorum oklahomense*. Algal Res. 67 https://doi.org/10.1016/j.algal.2022.102818.

Gatenby, C.M., Orcutt, D.M., Kreeger, D.A., Parker, B.C., Jones, V.A., Neves, R.J., 2003. Biochemical composition of three algal species proposed as food for captive freshwater mussels. J. Appl. Phycol. 15, 1–11.

Gautam, K., Waghmare, A., Soni, N., Teredesai, A.A., Shukla, M.R., Dasgupta, S., 2021. Algae protein enriched nutritious snacks and their sensory evaluation. J Food Sci Nutr Res 4. https://doi.org/10.26502/jfsnr.2642-11000073.

Giddings, T.H., Morphew, M.K., McIntosh, J.R., 2017. Preparing fission yeast for electron microscopy. Cold Spring Harb. Protoc. 2017, 69–73. https://doi.org/10.1101/pdb.prot091314.

Gonzalez-Gutierrez, J., Partal, P., Garcia-Morales, M., Gallegos, C., 2010. Development of highly-transparent protein/starch-based bioplastics. Bioresour. Technol. 101, 2007–2013. https://doi.org/10.1016/j.biortech.2009.10.025.

Gorissen, S.H.M., Crombag, J.J.R., Senden, J.M.G., Waterval, W.A.H., Bierau, J., Verdijk, L.B., van Loon, L.J.C., 2018. Protein content and amino acid composition of commercially available plant-based protein isolates. Amino Acids 50, 1685–1695. https://doi.org/10.1007/s00726-018-2640-5.

Hoekman, S.K., Broch, A., Robbins, C., Ceniceros, E., Natarajan, M., 2012. Review of biodiesel composition, properties, and specifications. Renew. Sustain. Energy Rev. 16, 143–169. https://doi.org/10.1016/j.rser.2011.07.143.

Huu, H. Do, 2016. Overview of the application of nucleotide in aquaculture. Journal of Coastal Life Medicine 4, 816–823. https://doi.org/10.12980/jclm.4.2016j6-165.

Krishnan, A., Cano, M., Burch, T.A., Weissman, J.C., Posewitz, M.C., 2020. Genome editing using Cas9-RNA ribonucleoprotein complexes in the high-productivity marine alga *Picochlorum celeri*. Algal Res. 49, 101944 https://doi.org/10.1016/j.algal.2020.101944.

Krishnan, A., Cano, M., Karns, D.A., Burch, T.A., Likhogrud, M., Aqui, M., Bailey, S., Verruto, J., Lambert, W., Kuzminov, F., Naghipor, M., Wang, Y., Ebmeier, C.C., Weissman, J.C., Posewitz, M.C., 2023. Simultaneous CAS9 editing of cpSRP43, LHCA6, and LHCA7 in *Picochlorum celeri* lowers chlorophyll levels and improves biomass productivity. Plant Direct 7. https://doi.org/10.1002/pld3.530.

Krishnan, A., Likhogrud, M., Cano, M., Edmundson, S., Melanson, J.B., Huesemann, M., McGowen, J., Weissman, J.C., Posewitz, M.C., 2021. *Picochlorum celeri* as a model system for robust outdoor algal growth in seawater. Sci. Rep. 11, 1–13. https://doi.org/10.1038/s41598-021-91106-5.

Laurens, L.M.L., Dempster, T.A., Jones, H.D.T., Wolfrum, E.J., van Wychen, S., McAllister, J.S.P., Rencenberger, M., Parchert, K.J., Gloe, L.M., 2012a. Algal biomass constituent analysis: method uncertainties and investigation of the underlying measuring chemistries. Anal. Chem. 84, 1879–1887. https://doi.org/10.1021/ac202668c.

Laurens, L.M.L., Quinn, M., Van Wychen, S., Templeton, D.W., Wolfrum, E.J., 2012b. Accurate and reliable quantification of total microalgal fuel potential as fatty acid methyl esters by in situ transesterification. Anal. Bioanal. Chem. 403, 167–178. https://doi.org/10.1007/s00216-012-5814-0.

Laurens, L.M.L., Wychen, S., Van Mcallister, J.P., Arrowsmith, S., Dempster, T.A., Mcgowen, J., Pienkos, P.T., 2014. Strain, biochemistry, and cultivation-dependent measurement variability of algal biomass composition. Anal. Biochem. 452, 86–95. https://doi.org/10.1016/j.ab.2014.02.009.

Lowry, O.H., Rosebrough, N.J., Farr, A.L., Randall, R.J., 1951. Protein measurement with the folin phenol reagent. Journal of Biological Chemistry 193C 265–275. https://doi.org/10.1016/S0021-9258(19)52451-6.

Luzon, D., 1948. Quantitative determination of carbohydrates with dreywood ' s anthrone reagent improved assembly of the hartung-clark double cannula for the isolated frog heart. Science (1979) 107, 254–255.

Lynas, M., Houlton, B.Z., Perry, S., 2021. Greater than 99% consensus on human caused climate change in the peer-reviewed scientific literature. Environ. Res. Lett. 16 https://doi.org/10.1088/1748-9326/ac2966.

Macleod, M., Arp, H.P.H., Tekman, M.B., Jahnke, A., 2021. The global threat from plastic pollution. Science (1979) 373, 61–65.

Mathiot, C., Ponge, P., Gallard, B., Sassi, J.F., Delrue, F., Le Moigne, N., 2019. Microalgae starch-based bioplastics: screening of ten strains and plasticization of unfractionated microalgae by extrusion. Carbohydr. Polym. 208, 142–151. https://doi.org/10.1016/j.carbpol.2018.12.057.

Mayorga, J., Flaig, D., Fuentes, G., Patricia, I.G., Cotabarren, J., David, W., 2021. Comparison of two strains of the edible cyanobacteria *Arthrospira*: biochemical characterization and antioxidant properties. Food Biosci. 42 https://doi.org/10.1016/j.fbio.2021.101144.

Mitra, S., Rauf, A., Tareq, A.M., Jahan, S., Emran, T. Bin, Shahriar, T.G., Dhama, K., Alhumaydhi, F.A., Aljohani, A.S.M., Rebezov, M., Uddin, M.S., Jeandet, P., Shah, Z. A., Shariati, M.A., Rengasamy, K.R., 2021. Potential health benefits of carotenoid lutein: an updated review. Food Chem. Toxicol. 154 https://doi.org/10.1016/j.fct.2021.112328.

Mohapatra, S., Ray, R.C., Ramachandran, S., 2018. Bioethanol from biorenewable feedstocks: technology, economics, and challenges. In: Bioethanol Production from Food Crops: Sustainable Sources, Interventions, and Challenges. Elsevier, pp. 3–27. https://doi.org/10.1016/B978-0-12-813766-6.00001-1.

Morris, D.L., 1948. Quantitative determination of carbohydrates with Dreywood's anthrone reagent. Science (1979 107, 254–255. https://doi.org/10.1126/science.107.2775.254.

Newell Arber, E.A., 1901. On the effect of nitrates on the carbon-assimilation of marine algae. Source: Ann. Bot. 15, 669–681.

Patel, A.K., Albarico, F.P.J.B., Perumal, P.K., Vadrale, A.P., Ntan, C.T., Chau, H.T.B., Anwar, C., Wani, H.M., din, ud, Pal, A., Saini, R., Ha, L.H., Senthilkumar, B., Tsang, Y.S., Chen, C.W., Dong, C., Di Singhania, R.R., 2022. Algae as an emerging

source of bioactive pigments. Bioresour. Technol. 351 https://doi.org/10.1016/j.biortech.2022.126910.

Phung Hai, T.A., Neelakantan, N., Tessman, M., Sherman, S.D., Griffin, G., Pomeroy, R., Mayfield, S.P., Burkart, M.D., 2020. Flexible polyurethanes, renewable fuels, and flavorings from a microalgae oil waste stream. Green Chem. 22, 3088–3094. https://doi.org/10.1039/d0gc00852d.

Porra, R.J., Thompson, W.A., Kriedemann, P.E., 1989. Determination of accurate extinction coefficients and simultaneous equations for assaying chlorophylls a and b extracted with four different solvents: verification of the concentration of chlorophyll standards by atomic absorption spectroscopy. Biochim. Biophys. Acta 975, 384–394.

Posewitz, M.C., Smolinski, S.L., Kanakagiri, S., Melis, A., Seibert, M., Ghirardi, M.L., 2004. Hydrogen photoproduction is attenuated by disruption of an isoamylase gene in *Chlamydomonas reinhardtii*. Plant Cell 16, 2151–2163. https://doi.org/10.1105/tpc.104.021972.

Procházková, G., Brányiková, I., Zachleder, V., Brányik, T., 2014. Effect of nutrient supply status on biomass composition of eukaryotic green microalgae. J. Appl. Phycol. 26, 1359–1377. https://doi.org/10.1007/s10811-013-0154-9.

Ran, W., Wang, H., Liu, Y., Qi, M., Xiang, Q., Yao, C., Zhang, Y., Lan, X., 2019. Storage of starch and lipids in microalgae: biosynthesis and manipulation by nutrients. Bioresour. Technol. https://doi.org/10.1016/j.biortech.2019.121894.

Ricketts, T.R., 1966. On the chemical composition of some unicellular algae. Phytochemistry 5, 67–76. https://doi.org/10.1016/S0031-9422(00)85082-7.

Rony, Z.I., Mofijur, M., Hasan, M.M., Ahmed, S.F., Badruddin, I.A., Khan, T.M.Y., 2023. Conversion of algal biomass into renewable fuel: a mini review of chemical and biochemical processes. Front. Energy Res. 11 https://doi.org/10.3389/fenrg.2023.1124302.

Ruiz, J., Olivieri, G., De Vree, J., Bosma, R., Willems, P., Reith, J.H., Eppink, M.H.M., Kleinegris, D.M.M., Wijffels, R.H., Barbosa, M.J., 2016. Towards industrial products from microalgae. Energy Environ. Sci. 9, 3036–3043. https://doi.org/10.1039/c6ee01493c.

Schertz, F.M., 1927. Commercial applications of chlorophyll derivatives. Ind. Eng. Chem. 19.

Suastes-Rivas, J.K., Hernández-Altamirano, R., Mena-Cervantes, V.Y., Barrios Gómez, E. J., Chairez, I., 2020. Biodiesel production, through intensification and profitable distribution of fatty acid methyl esters by a microalgae-yeast co-culture, isolated from wastewater as a function of the nutrients' composition of the culture media. Fuel 280. https://doi.org/10.1016/j.fuel.2020.118633.

Thombare, N., Jha, U., Mishra, S., Siddiqui, M.Z., 2016. Guar gum as a promising starting material for diverse applications: a review. Int. J. Biol. Macromol. 88, 361–372. https://doi.org/10.1016/j.ijbiomac.2016.04.001.

Van Wychen, S., Rowland, S.M., Lesco, K.C., Shanta, P.V., Dong, T., Laurens, L.M.L., 2021. Advanced mass balance characterization and fractionation of algal biomass composition. J. Appl. Phycol. 33, 2695–2708. https://doi.org/10.1007/s10811-021-02508-x.

Viles, F.J., Silverman, L., 1949. Determination of starch and cellulose with anthrone. Anal. Chem. 21, 950–953. https://doi.org/10.1021/ac60032a019.

Waslien, C.I., Calloway, D.H., Margen, S., Costa, F., 1970. Uric acid levels in men fed algae and yeast as protein sources. J. Food Sci. 35.

Weissman, J.C., Goebel, R.P., 1987. Factors affecting the photosynthetic yield of microalgae. In: FY 1986 Aquatic Species Program Annual Report, pp. 139–168. SERI/SP-231-3071, Golden, CO.

Weissman, J.C., Likhogrud, M., Thomas, D.C., Fang, W., Karns, D.A.J., Chung, J.W., Nielsen, R., Posewitz, M.C., 2018. High-light selection produces a fast-growing *Picochlorum celeri*. Algal Res. 36, 17–28. https://doi.org/10.1016/j.algal.2018.09.024.

Wijffels, R.H., Barbosa, M.J., 2010. An outlook on microalgal biofuels. Science (1979 329, 793–796. https://doi.org/10.1126/science.1189139.

Work, V.H., Bentley, F.K., Scholz, M.J., D'Adamo, S., Gu, H., Vogler, B.W., Franks, D.T., Stanish, L.F., Jinkerson, R.E., Posewitz, M.C., 2013. Biocommodities from photosynthetic microorganisms. Environ. Prog. Sustain. Energy 32, 989–1001. https://doi.org/10.1002/ep.11849.

Work, V.H., Radakovits, R., Jinkerson, R.E., Meuser, J.E., Elliott, L.G., Vinyard, D.J., Laurens, L.M.L., Dismukes, G.C., Posewitz, M.C., 2010. Increased lipid accumulation in the *Chlamydomonas reinhardtii* sta7-10 starchless isoamylase mutant and increased carbohydrate synthesis in complemented strains. Eukaryot. Cell 9, 1251–1261. https://doi.org/10.1128/EC.00075-10.

Wu, Y., Li, W., Cui, W., Eskin, N.A.M., Goff, H.D., 2012. A molecular modeling approach to understand conformation-functionality relationships of galactomannans with different mannose/galactose ratios. Food Hydrocolloids 26, 359–364. https://doi.org/10.1016/j.foodhyd.2011.02.029.

Xi, X., Pizzi, A., Gerardin, C., Du, G., 2019. Glucose-biobased non-isocyanate polyurethane rigid foams. J Renew Mater 7, 301–312. https://doi.org/10.32604/jrm.2019.04174.

Zea Obando, C., Linossier, I., Kervarec, N., Zubia, M., Turquet, J., Faÿ, F., Rehel, K., 2016. Rapid identification of osmolytes in tropical microalgae and cyanobacteria by 1H HR-MAS NMR spectroscopy. Talanta 153, 372–380. https://doi.org/10.1016/j.talanta.2016.02.024.